Accepted Manuscript

A sequential cycloaddition strategy for the synthesis of Alsmaphorazine B traces a path through a family of *Alstonia* alkaloids

Allen Y. Hong, Christopher D. Vanderwal

PII: S0040-4020(16)31136-X

DOI: 10.1016/j.tet.2016.11.004

Reference: TET 28218

To appear in: *Tetrahedron*

Received Date: 1 September 2016

Revised Date: 4 October 2016

Accepted Date: 1 November 2016

Please cite this article as: Hong AY, Vanderwal CD, A sequential cycloaddition strategy for the synthesis of Alsmaphorazine B traces a path through a family of *Alstonia* alkaloids, *Tetrahedron* (2016), doi: 10.1016/j.tet.2016.11.004.

Graphical Abstract

A Sequential Cycloaddition Strategy for the Synthesis of Alsmaphorazine B Traces a Path through a Family of *Alstonia* Alkaloids

Leave this area blank for abstract info.

Allen Y. Hong, Christopher D. Vanderwal**
Department of Chemistry, 1102 Natural Sciences II, University of California, Irvine, California 92697-2025, USA

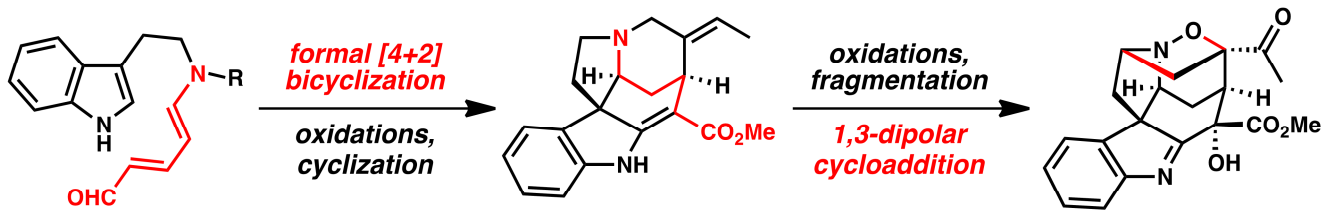

Zincke aldehyde *akuammicine* *alsmaphorazine B*

Tetrahedron
journal homepage: www.elsevier.com

A Sequential Cycloaddition Strategy for the Synthesis of Alsmaphorazine B Traces a Path Through a Family of *Alstonia* Alkaloids

Allen Y. Hong[a*], Christopher D. Vanderwal[a*]

[a]*Department of Chemistry, 1102 Natural Sciences II, University of California, Irvine, California 92697-2025, USA*

ARTICLE INFO

Article history:
Received
Received in revised form
Accepted
Available online

Keywords:
Cycloaddition
Oxidation
Alkaloids
Total Synthesis
Natural Products

ABSTRACT

Driven by a new biogenetic hypothesis, the first total synthesis of alsmaphorazine B and several related indole alkaloids has been achieved. Numerous early approaches proved unsuccessful owing to unproductive side reactivity; nevertheless, they provided important clues that guided the evolution of our strategy. Critical to our success was a major improvement in our Zincke aldehyde cycloaddition strategy, which permitted the efficient gram-scale synthesis of akuammicine. The sequential chemoselective oxidations of akuammicine leading up to the key oxidative rearrangement also yielded several biogenetically related indole alkaloids *en route* to alsmaphorazine B.

*Corresponding authors: hong.allen@gene.com, cdv@uci.edu

1. Introduction and Background

The alsmaphorazine alkaloids (Figure 1) were isolated by Morita and co-workers[1] from *Alstonia pneumatophora*, a tree native to Southeast Asia. In the only bioassay reported to date on these compounds, these workers found that alsmaphorazine A (**1**) inhibits nitric oxide production *in vivo* (IC_{50} = 49.2 μM), but alsmaphorazine B (**2**) was inactive. The alsmaphorazines feature a stereochemically dense, highly oxidized, and caged hexacyclic skeleton with an endocyclic N–O bond. The caged ring system features several embedded heterocycles: a 1,2-oxazinane, a 1,2-oxazolidine, and a pyrrolidine. This arrangement is rare among indole alkaloids and prompted questions about its likely biosynthetic origin.

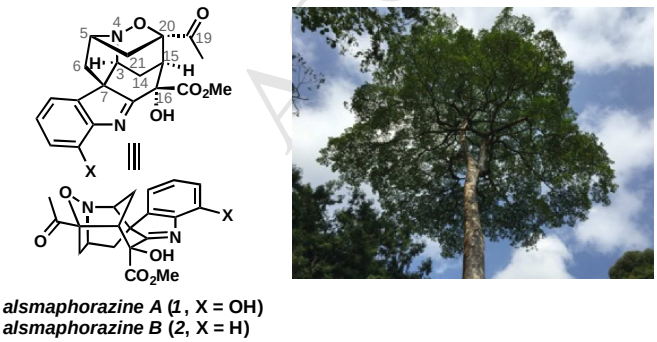

Figure 1. Alsmaphorazines from *Alstonia pneumatophora*.

The key question of whether enzymes can catalyze cycloaddition reactions, particularly 1,3-dipolar cycloaddition reactions, has intensified in recent years. A combination of

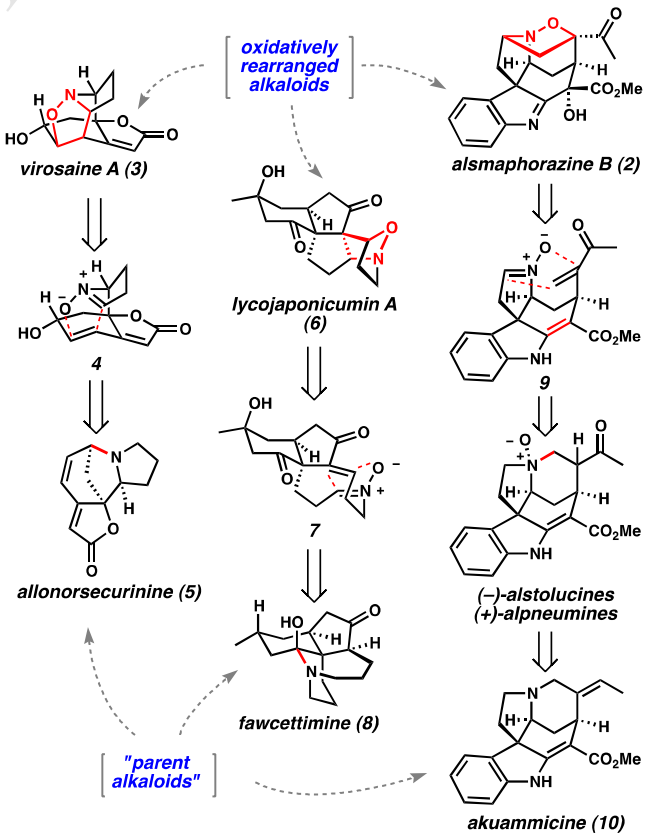

Scheme 1. Postulated Origin of Alsmaphorazines and other Naturally Occurring Alkaloids.

computational[2] and total synthesis[3] studies have shed some light on the proposed cycloaddition steps leading to oxidized *Securinega* and *Lycopodium* alkaloids (Scheme 1), which are believed to arise from nitrone-alkene dipolar cycloadditions. More recently, a compelling example of an the first known enzyme-catalyzed dipolar cycloaddition was reported by Leys and co-workers.[4]

Our new hypothesis for the biosynthetic origin of the alsmaphorazines differed from the proposed biosynthetic origin put forth by Morita and coworkers,[1] in which an alternative oxidation and rearrangement sequence takes place through epoxide and *N*-oxide intermediates. In its initial form, our hypothesis included only the nitrone/alkene cycloaddition and vinylogous carbamate hydroxylation steps (**9** to **2**), but it eventually extended further in the direction of other *Alstonia* alkaloids, ending at akuammicine. The evolution of this hypothesis and the strategy based upon it is described in detail in this report.

2. Synthetic Plan

2.1. Retrosynthetic Analysis

The N–O bond shared by the isoxazolidine and oxazinane rings and integral to the caged polycyclic framework is an unusual feature of the alsmaphorazines that must be the focus of any synthesis design. We reasoned that the 1,2-oxazolidine ring might be accessed by a nitrone-alkene 1,3-dipolar cycloaddition (Scheme 2), and that the tertiary alcohol at C16 should arise via oxidation of the vinylogous carbamate in **9**. Further simplification of the proposed cycloaddition substrate through a series of oxidations and incorporation of a four-carbon fragment pointed to tetracyclic indoline **13** as an attractive precursor, which would be accessible from our Zincke aldehyde cycloaddition methodology.[5] Ultimately, our synthesis would begin from tryptamine and pyridine derivatives as simple, readily accessible precursors.

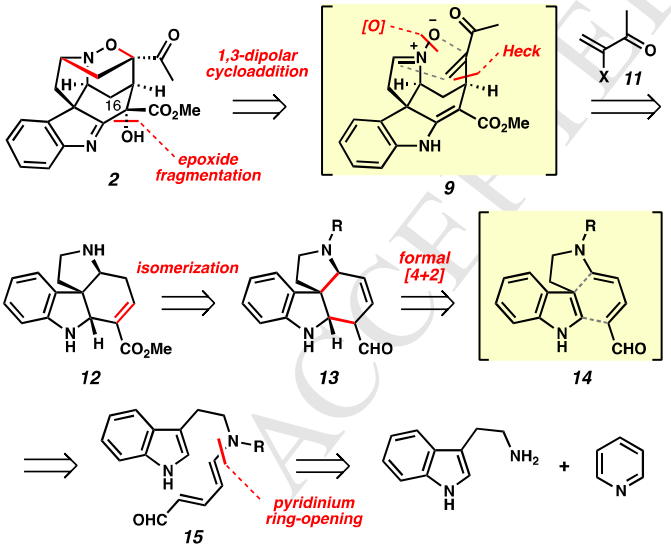

Scheme 2. Retrosynthetic Analysis of Alsmaphorazine B (**2**).

We therefore divided our synthetic strategy into two key architecture-building stages: indole-Zincke aldehyde anionic formal [4+2] cycloaddition and nitrone-alkene 1,3-dipolar cycloaddition. These two major events would be separated by execution of our oxidation state adjustments, which would be just as critical in the execution of the synthetic design.

3. Results and Discussion

3.1. Construction of the Tetracyclic Alkaloid Core by Anionic [4+2] Bicyclization

The combination of *N*(4)-substituted tryptamines with Zincke salts[6,7] proved to be a powerful and direct method for the construction of the key Zincke aldehyde intermediates employed in our past syntheses of polycyclic indole alkaloids.[5] While this method served us well in numerous contexts, we continued to look for complementary methods that would address some of the key synthetic limitations. The key problems posed by the Zincke salt method as depicted in Scheme 3 included: (1) the required use of excess tryptamine component for full conversion to Zincke aldehyde product; (2) the necessary chromatographic and activated charcoal purification of the Zincke aldehyde for efficient cyclization in the next step; and (3) lower than desired overall yields and scalability for the critical two-step sequence. As a result, we sought to improve reaction stoichiometry and yields while simplifying operations and purification for efficient scale-up. We selected the method of Marazano[8] featuring the alternative use of potassium glutaconaldehyde for comparison.

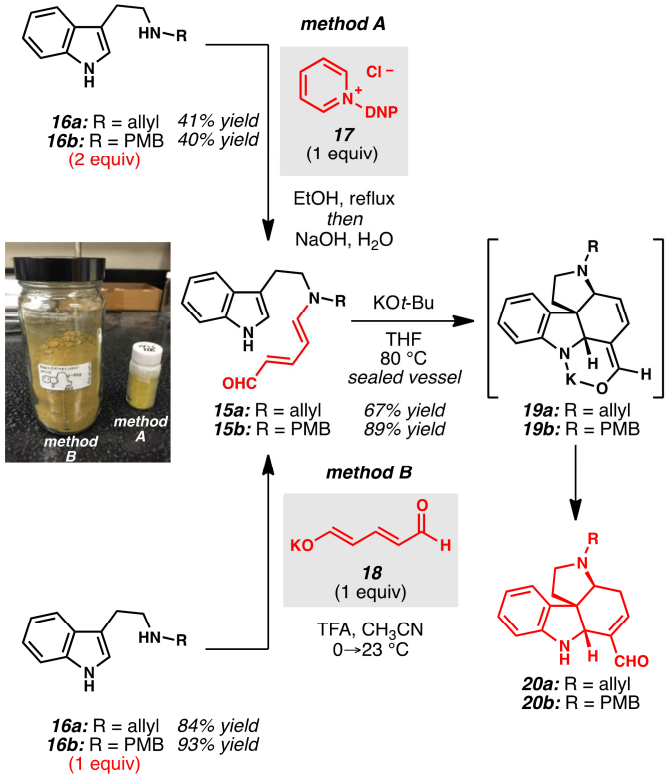

Scheme 3. Zincke Aldehyde Formation and Formal [4+2] Anionic Bicyclization.

Preparation of the *N*(4)-substituted tryptamines was achieved either by using the tryptophyl fragment as the electrophilic component in an S_N2 reaction[5b,d] or the nucleophilic component in reductive amination.[5a,d] In this manner, we prepared *N*-allyl tryptamine **16a** and *N*-PMB tryptamine **16b** in good yields. These tryptamines were typically used crude in the subsequent Zincke aldehyde formation (Scheme 3).

Combination of these tryptamines with Zincke salts in EtOH at 80 °C followed by hydrolysis provided the corresponding Zincke aldehydes **15a** and **15b** in 41% and 40% yield, respectively (with respect to the tryptamine component, with high yield with respect to the Zincke salt, and good recovery of the mass balance of the amine).

When we applied Marazano's protocol[8] in the synthesis of the same Zincke aldehydes using TFA and potassium glutaconaldehyde in CH_2Cl_2 at ambient temperature, we observed smooth conversion to the desired product (Scheme 3). However, we found contamination with a highly colored unidentified red impurity. Substituting the CH_2Cl_2 with CH_3CN as the reaction solvent improved the reaction by reducing the dark coloration of the product. Initiating the reaction at 0 °C also proved beneficial, and in this manner, we were able to achieve a 84–93% yield over two steps relative to the tryptamine component. More importantly, the purification process was greatly simplified. Aqueous work-up, sonication and precipitation of solid product from Et_2O followed by filtration enables a convenient method for isolation of Zincke aldehyde product for use in the subsequent anionic bicyclization step. When compared to the Zincke salt method, this represents a two-fold increase in yield, and as a result, quickly became the preferred method for preparing the large amounts of material needed for the planned alsmaphorazine synthesis.

With the key Zincke aldehyde in hand, we were able to perform the anionic [4+2] bicyclization[5a,9] by combination with KO*t*-Bu in a sealed pressure vessel heated to 80 °C (Scheme 3). The *N*-PMB substrate provided a superior yield of *N*-PMB tetracyclic enal product **20b** (89% yield) compared with the analogous *N*-allyl substrate **20a** (63% yield). However, based on our previous studies, it was unclear if we would be able to remove the PMB group at a later stage,[5] so we processed material with both *N*-allyl and *N*-PMB protecting groups in place.

For the synthesis of the alsmaphorazines, the incorporation of an aminodienoic ester in place of the aminopentadienal (Zincke aldehyde) would improve synthetic efficiency. We were able to construct the ester analogs of **15a** and **15b** (not shown), but the cyclization reaction proved unsuccessful under numerous conditions, highlighting the importance of the more electron-deficient aldehyde in the [4+2] anionic bicyclization.

With tetracyclic enal compounds in hand, we reasoned that we could begin oxidation state adjustment of the tetracyclic core to progress toward the alsmaphorazine alkaloids. To improve the stability of our synthetic intermediates, we aimed to convert the enal into the more robust unsaturated methyl ester found in the natural product target.

Examples of direct oxidative esterifications of enals to unsaturated esters are relatively common in the literature, but we were unsure of the functional group compatibility problems posed by our system (Scheme 4). Indeed, applying Corey–Ganem oxidation conditions (NaCN, AcOH, MeOH)[10] or NHC-catalyzed oxidations[11] provided little or no desired product. Less common conditions such as I_2/MeOH, TCCA/MeOH,[12] oxone/MeOH,[13] and vanadium catalysis[14] proved unsuccessful as well. A sequential approach to this oxidation through an intermediate carboxylic acid using the Lindgren–Kraus–Pinnick oxidation was equally untenable. We suspected that one key challenge to this direct oxidation was the competitive oxidation of the indoline nitrogen, because similar reactivity problems have been reported.[15]

To expedite the investigation of downstream chemistry, we resorted to protection of the indoline as an *N*-Boc carbamate. Treatment of tetracyclic indolines **20a** and **20b** with Boc_2O in 1,2-DCE at 80 °C in a sealed vessel[5d] provided carbamates **22a** and **22b**. Conveniently, we found that the addition of methanol led to the precipitation of product from the solution, and filtration afforded the desired *N*-Boc tetracyclic enal. Subsequent Lindgren oxidation[16] afforded an intermediate carboxylic acid. Methylation could be achieved with TMS diazomethane or diazomethane in Et_2O/MeOH or DBU/CH_3I in CH_3CN, providing the target methyl ester in good yield, but we preferred the latter conditions for more convenient scale-up and for safety considerations.

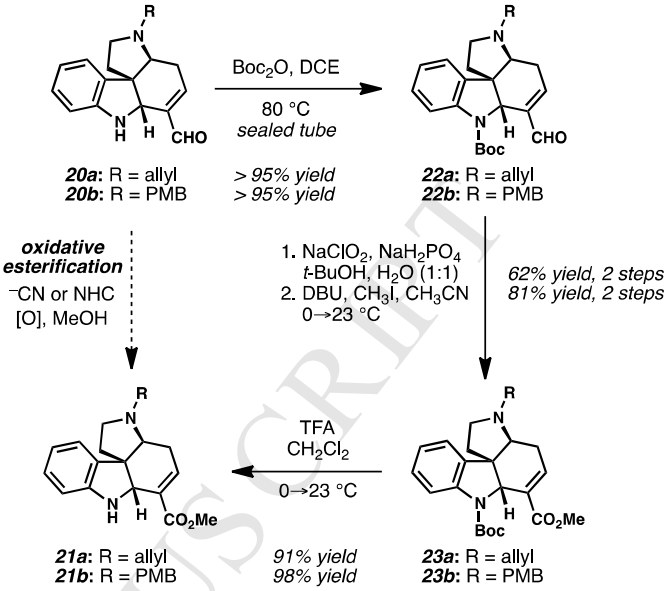

Scheme 4. Oxidative Esterification of Tetracyclic Enals.

3.2. Intermolecular Heck Strategy Toward Dipolar Cycloaddition Substrates

With the key tetracycle formed by a formal [4+2] cycloaddition, we turned our attention to the next cyclization event: the nitrone-alkene dipolar cycloaddition.[17] The precise sequence of events to construct the key reactive functionality was not clear to us at the outset, and we believed our best chance of reaching our goal was through an intermolecular Heck reaction.[18] Based on examples of tertiary amines as directing groups in the Heck literature,[19] we anticipated that the amine might guide a diastereoselective Heck insertion to give the desired product, with the Heck donor delivered to the more hindered, concave face of the acceptor (Scheme 5). Subsequent tertiary amine deprotection and oxidation along with masked allylic alcohol functional group modification would afford the desired nitrone and alkene partners for the key dipolar cycloaddition.

Our intermolecular Heck efforts began with enals **20** or esters **21**. Both substrates, as well as their *N*-Boc carbamates **22** and **23** were evaluated as substrates for C–C bond formation. We investigated vinyl iodides such as **24** and **25** as donors. Despite the evaluation of numerous palladium precatalyst and ligand combinations, we observed only complex reaction mixtures without any hints of productive reactivity. The vinyl halide components were typically consumed during the reaction, but the enal or enoate partners reacted slowly if at all. Our combined studies suggest that the Heck reaction may be limited by the steric bulk of the concave polycyclic system as well as competitive decomposition of vinyl halide intermediates. With our lack of initial success, we evaluated other approaches in parallel with this first strategy.

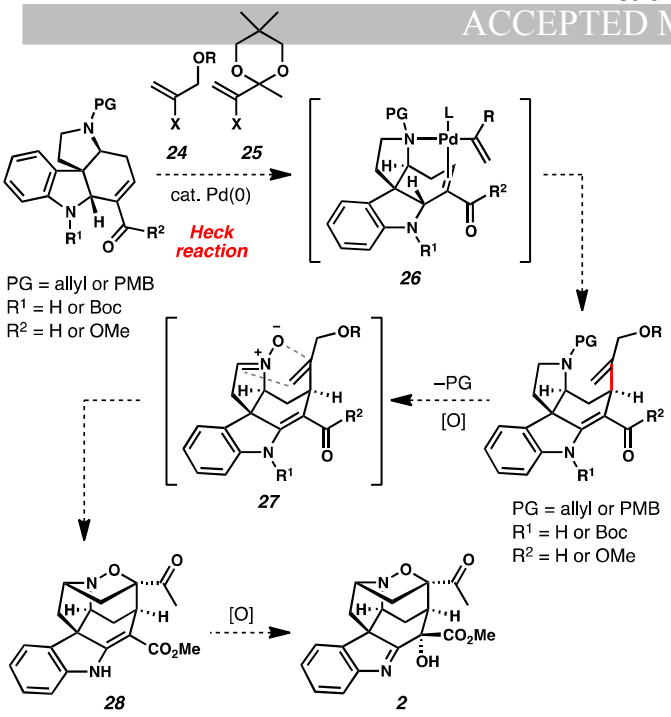

Scheme 5. Intermolecular Heck Strategy.

3.3. Tetracycle Functionalization for Cyclization Strategies

With the challenges posed by the intermolecular Heck approach, we turned our attention to intramolecular variants of this venerable reaction.[18] This fact would allow us to deliver the key functionality where needed and reduce reactivity and steric problems that might have hindered our first approach. Refunctionalization of the tetracyclic core would certainly be needed to set up the next phase of our revised synthetic plan (Scheme 6).

Removal of the *N*-allyl group in **23a** could be effected by treatment with catalytic amounts of $Pd(PPh_3)_4$ and 5-methyl Meldrum's acid in CH_3CN at 0 °C,[5b,d] while removal of the *N*-PMB group in **23b** could be achieved by treatment with DDQ in CH_2Cl_2/H_2O or CAN in CH_3CN. The intermediate secondary amine is typically used crude after the allyl cleavage reaction, but can be isolated from the PMB cleavage reaction by column chromatography in 62% yield or treated with an electrophile as a crude solution for further transformation to useful intermediates. In this manner, we were able to prepare numerous derivatives of our tetracyclic core by appendage of different side chains: *O*-acyl hydroxylamine (**30a**) as well as allylic amines **30b**, **30c**, **30d**, **30e, 30f** and propargylic amine **30g**. In addition, conjugate adducts **30h** and **30i** could also be forged.

These new tetracycles would prove important in our forward progress toward alsmaphorazine B as discussed below. While not all of them would lead us to our key targets, they nevertheless taught us much about the preferred reactivity of the polycyclic core and guided the evolution of our strategy.

3.4. N–O Tethered Intramolecular Heck Strategy Toward Dipolar Cycloaddition Substrates

As an alternative approach featuring earlier installation of the key N–O bond present in the natural product, we next envisioned an intramolecular Heck strategy with an N–O bond-containing tether (Scheme 7). We expected that the Heck cyclization would tolerate this potentially sensitive functionality and forge a new 7-membered ring.[20] Subsequent oxidation of the hydroxylamine

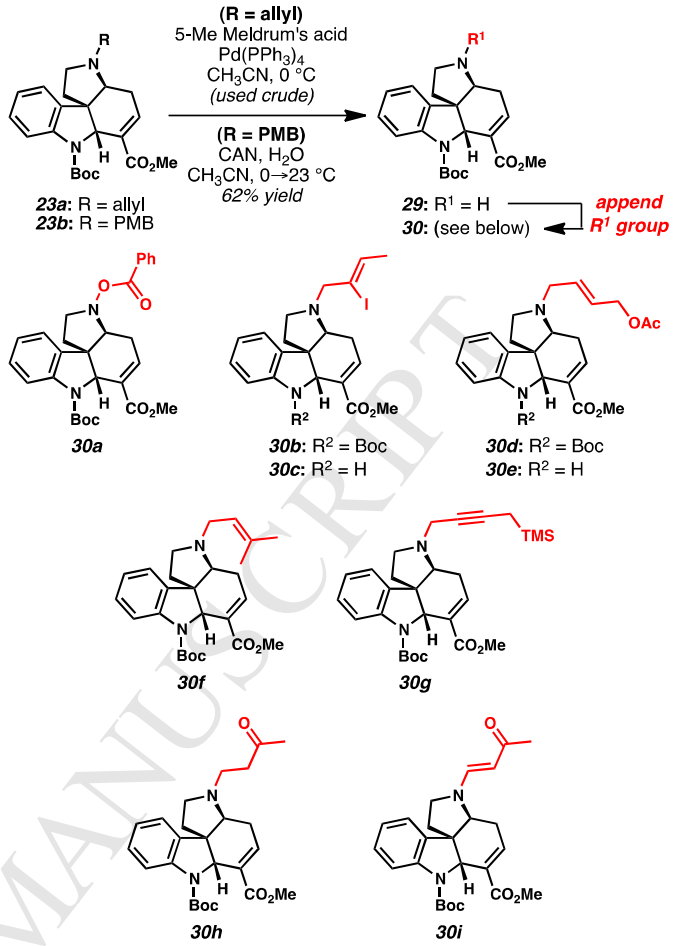

Scheme 6. Synthesis of Functionalized Tetracycles.

would trigger a cascade process in which the N–O bond would fragment to a nitrone and an allylic alcohol,[21] providing a basis for the planned 1,3-dipolar cycloaddition leading to the hexacyclic alsmaphorazine core.

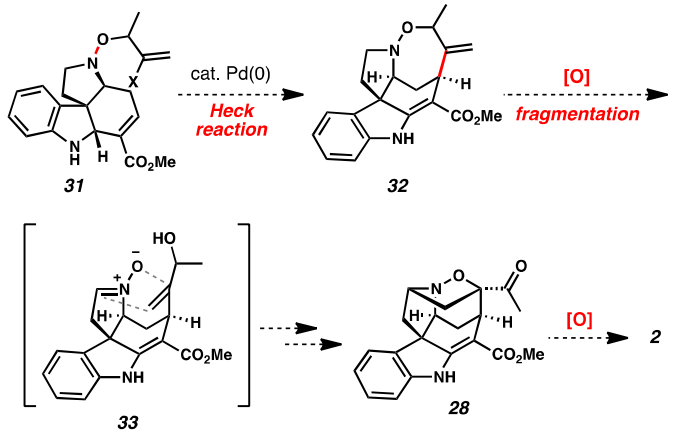

Scheme 7. N–O Tethered Intramolecular Heck Strategy.

To begin the tether construction for the study of this route, secondary amine **29** was treated with benzoyl peroxide[22] to form *O*-benzoyl hydroxylamine product **30a** (Scheme 8). Subsequent ester cleavage was straightforward in the presence of hydroxide base; however, the isolated material lacked two key signals in the ^{13}C NMR corresponding to the C=C bond of the enoate and

showed a shift in the carbonyl resonance. We reasoned that the liberated hydroxylamine cyclized in an oxa-Michael fashion to provide an undesired pentacycle, which is analogous to several structures reported by Robinson and Kuehne (**36** and **37**, respectively).[23] Despite this setback, we sought another route to evaluate the N–O tethered intramolecular Heck strategy we had planned.

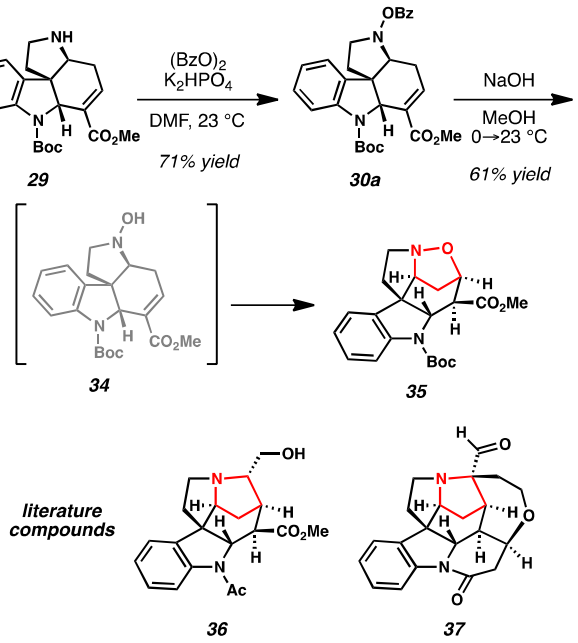

Scheme 8. Undesired Oxy-Michael Addition During Attempts to Prepare N–O Tethered Intramolecular Heck Substrate.

We envisioned that the installation of a vinyl halide-containing side chain followed *N*-oxidation and a [2,3]-Meisenheimer rearrangement[24] would provide the requisite Heck substrate (Scheme 9A). Tetracycle **30c** bearing vinyl iodide was prepared by deprotection and refunctionalization as described above (Scheme 6). Oxidation of the unprotected indoline primarily led to hydroxylamine **38** and nitrone **39** in low yield. This experiment suggested that a protecting group was important for directing oxidation to the *N*(4) nitrogen.

Subsequent oxidation of *N*-Boc indoline **30b** with various reagents led to complex reaction mixtures and incomplete conversion, suggesting that the transformation would be more challenging than we originally anticipated. To simplify the problem and probe the mechanistic pathway of the reaction, we explored the same transformation with a simplified *N*-allyl substrate **23a** for ease of product analysis (Scheme 9B).

Oxidation of *N*-allyl compound **23a** led to a complex mixture that contained residual starting material. *N*-Oxidation likely occurred, but LCMS analysis of the reaction mixture indicated the formation of a compound with the mass of the intermediate *N*-oxide or hydroxylamine and two compounds bearing the mass of the nitrone. Analysis of the crude reaction mixture by ^{1}H NMR showed the presence of many more alkene peaks that did not exhibit a simple allyl pattern, which might be rationalized by a Cope elimination leading to an extended π-systems present in fragmentation products **41**, **42**, and **43**. It was clear that the Meisenheimer rearrangement in particular and early stage N–O bond installation in general was proving enormously challenging; therefore, we devised alternative strategies to help us achieve our goal of completing alsmaphorazine B.

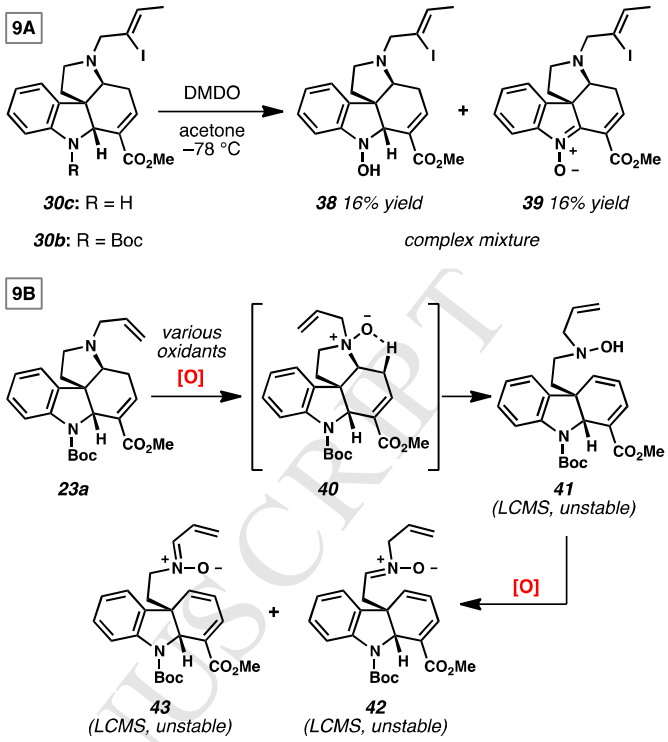

Scheme 9. Plausible Mechanism for Cope Elimination and Fragmentation of Tetracyclic Indolines.

3.5. Biomimetic Synthesis of Numerous Alkaloids from Akuammicine by Late-Stage Biomimetic Oxidation and Rearrangement

Clearly, several intermolecular and intramolecular Heck strategies and early stage oxidation approaches led to unexpected reactivity that limited our ability to advance toward the key nitrone/alkene dipolar cycloaddition. At this point, we drew inspiration from the structure of the natural product itself in planning the next stages of our synthetic design.

Upon review of biogenetically related natural products co-isolated from the *Alstonia* plants, we outlined a new proposal for a biosynthetic pathway leading to alsmaphorazine B from akuammicine, a well-known alkaloid at a lower oxidation state (Scheme 10). The route we designed would proceed through intermediate alkaloids containing alcohols, epoxides, ketones, and *N*-oxides. While the endpoints of this pathway mirror those suggested by Morita in his isolation report,[1] the intermediates and transformations differ considerably. We valued this approach because we could check our progress by comparison with known *Alstonia* alkaloids such as the alstolucines[25] and the alpneumines[26] with intermediate levels of oxidation.

We initially considered interception of our hypothetical biogenesis at the stage of alstolucine B (**46**) or its C20 epimer, alstolucine F. We envisioned that the methyl ketones of these natural products could arise from a sequential Michael cascade or Rauhut–Currier type reaction.

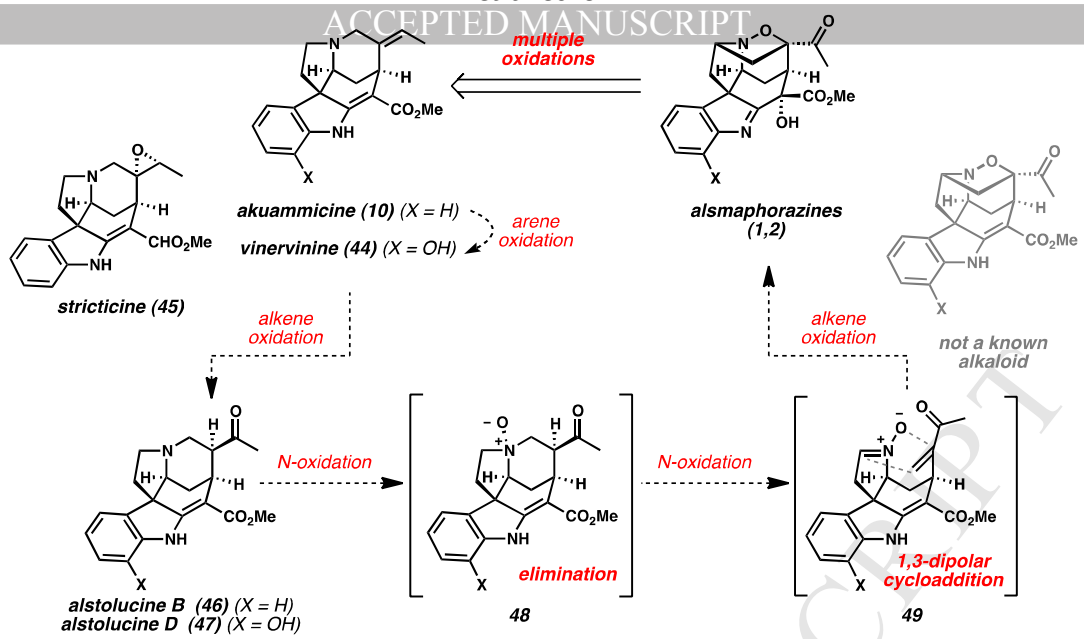

Scheme 10. Proposed Biosynthetic Pathway from Akuammicine to Alsmaphorazines.

Our deprotection and refunctionalization approach once again enabled us to functionalize our tetracyclic core to test this hypothesis by trapping secondary amine **29** with methyl vinyl ketone (Schemes 6 and 11).[27] A second Michael addition of the ketone **30h** to the proximal unsaturated ester[28] would complete the caged structure of the intermediate ketones in our synthetic pathway. However, despite evaluation of numerous bases for the cyclization event, we did not observe cyclization and instead saw only elimination product or recovered starting material.

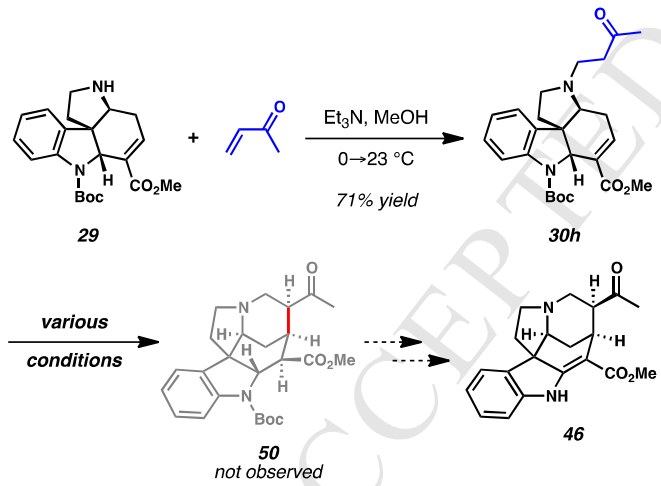

Scheme 11. Conjugate Addition Strategy Toward Ketone **46**.

While this challenging cyclization led to some setbacks, we nevertheless were convinced in the importance of the pentacyclic methyl ketone **46** or congeners at a higher oxidation state as key synthetic intermediates that would enable a successful synthesis. Another option for arriving at the same ketone intermediate was planned by taking advantage of an unsaturated vinylogous amide analog **30i** (Scheme 12). We anticipated that direct palladation could provide a vinylpalladium species which could undergo a Heck reaction with the adjacent unsaturated ester.[29] Following reductive elimination, we expected that the caged ring system would be formed. Hydrogenation of the less substituted vinylogous amide could provide the target pentacyclic ketone **46**. Unfortunately, we never observed the desired cyclization product under numerous reported conditions and we became unsure about the ease of palladation and the ring strain in the cyclization product.

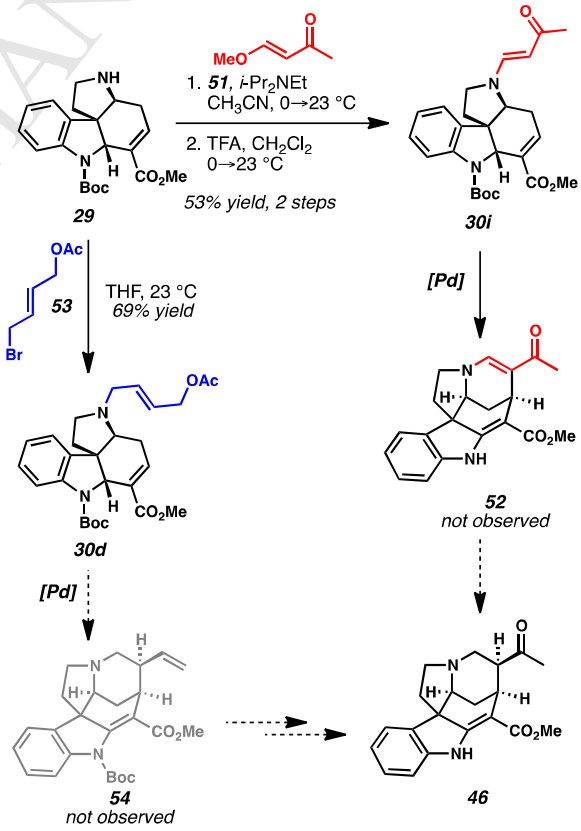

Scheme 12. Oxidative and π-Allyl Heck and Cyclization Strategies to Ketone **46**.

An alternative Heck strategy was also envisioned from allylic acetate **30d** (Scheme 6). A π-allyl Heck reaction[30] followed by Wacker-type functionalization of the vinyl group could lead to the desired methyl ketone **46** (Scheme 12). This compound was formed in a straightforward fashion by a similar deprotection and refunctionalization sequence with allylic bromide allylic acetate

53 (Scheme 6). With this compound in hand, we evaluated numerous palladium precatalysts but cyclization was not observed; instead only decomposition of the starting material occurred after long reaction times.

We finally decided to test our biomimetic proposal from the beginning, with the *Strychnos* alkaloid akuammicine, adapting our earlier approach to related alkaloids.[5] Our one-pot deprotection/refunctionalization procedure provided tetracyclic vinyl iodide **30d** (Scheme 6). Following the strategy first pioneered by Rawal,[31,33g] and used more recently by MacMillan[33g] and Andrade,[33f,h,i,j] treatment of this compound with $Pd(OAc)_2$ and PPh_3 in Et_3N with heating led to a successful intramolecular Heck reaction to form akuammicine (**10**) in nearly quantitative yield (Scheme 13).[32,33] Our synthetic route to akuammicine proceeded in 39% yield from commercially available tryptamine. This reaction provided gram-quantities of the alkaloid and therefore facilitated the next phase in our studies, the oxidative rearrangement of akuammicine to alsmaphorazine B via several known alkaloids. Based on the limited knowledge of late-stage alkaloid oxidation, this quantity of material would certainly be needed to balance the risk of this approach.

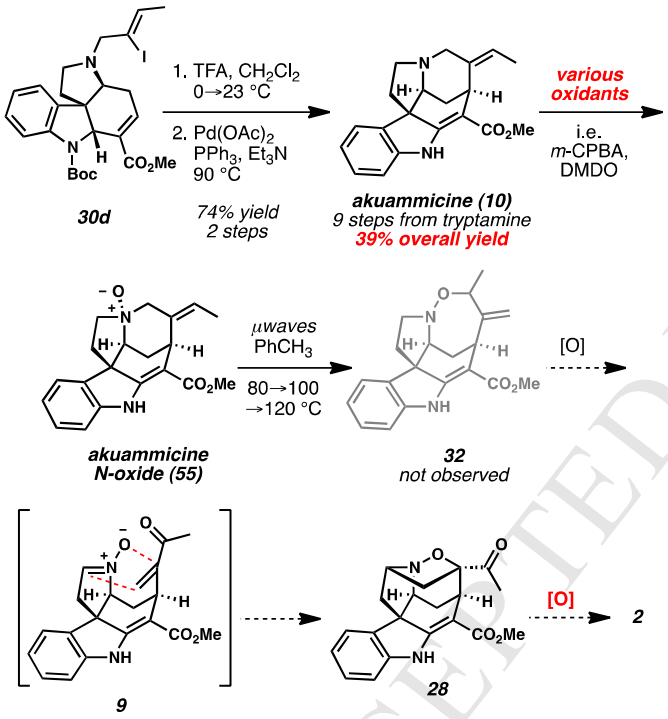

Scheme 13. Initial Double Oxidation Strategy.

With ample quantities of akuammicine in hand, we were poised to evaluate our proposed biomimetic oxidative rearrangement sequence for construction of the alsmaphorazines. Attempted double oxidation of akuammicine led to akuammicine *N*-oxide (**55**),[34] which was strongly deactivated to further oxidation at the trisubstituted alkene (Scheme 13). More aggressive oxidation conditions led only to intractable mixtures arising from decomposition. With this *N*-oxide compound, however, we reasoned that we could take advantage of a Meisenheimer rearrangement to provide a handle for our planned nitrone-alkene 1,3-dipolar cycloaddition. While a sigmatropic [2,3]-Meisenheimer rearrangement seemed conformationally implausible owing to the caged structure, a radical [1,2]-Meisenheimer rearrangement[35] held much more promise. Heating of the *N*-oxide did not provide any detectable product of the desired rearrangement and instead led to decomposition when the reaction was pushed to full conversion.

The direct conversion of the trisubstituted alkene of akuammicine to the corresponding methyl ketones **46** or **56** was an equally attractive starting point (Scheme 14). Toward this end, we subjected the compound to Wacker oxidation conditions, transition metal-catalyzed or standard hydroboration/oxidation, thiol-ene/Pummerer, oxymercuration, and Mukaiyama hydration/oxidation, but none of these options were successful; rather, they either proved unreactive, proceeded with undesired regioselectivity, or led to complex reaction mixtures.

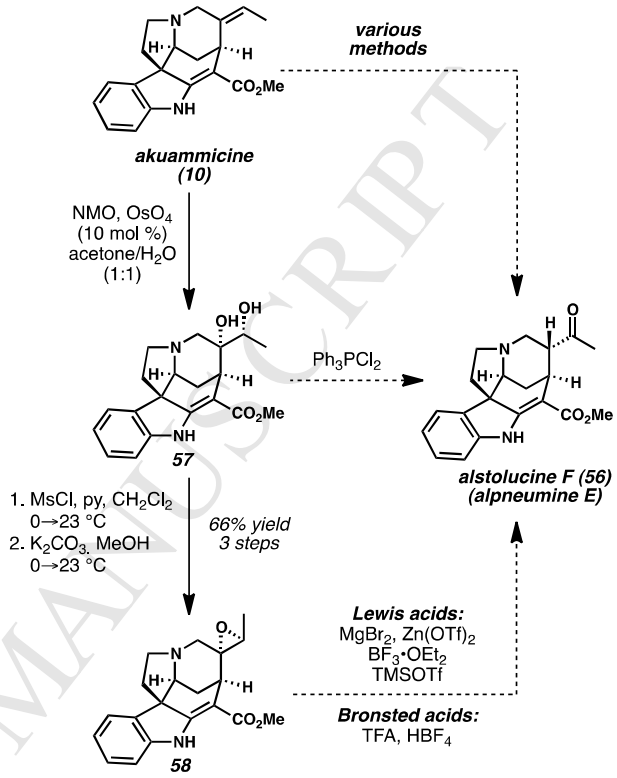

Scheme 14. Attempted Redox Isomerization of Epoxide **58** and Diol **57** to Ketone **56**.

Without a direct option, we opted to prepare pentacyclic ketone **56** by rearrangement of the isomeric epoxide **58** (Scheme 14). Chemoselective dihydroxylation of akuammicine (**10**) proceeded using standard Upjohn conditions.[36,37,38] We subjected this key diol **57** to known redox isomerization conditions using Ph_3PCl_2.[39] Rearrangement by means of a stereospecific hydride shift was expected to provide the desired ketone. Despite various modifications of the conditions, we were unable to obtain ketone product **56**. We suspected that the reactive nature of the reagent might not be compatible with the abundance of Lewis basic functionality present in our molecule.

While diol rearrangement did not provide a path forward, we sought to perform a similar rearrangement using an epoxide via a Meinwald rearrangement. Following the precedent of Le Men,[38] we performed a selective alcohol mesylation and internal displacement to construct epoxide **58** (Scheme 14). With this compound in hand, we evaluated a number of Lewis acids for the formation of ketone **56**, without success.

Taking a more step-wise approach (Scheme 15), we began with a citric acid-modified dihydroxylation procedure developed by Fokin and Sharpless.[40] This procedure proved superior to the Upjohn conditions that we used initially owing to the relative ease of reaction work up and elimination of troublesome

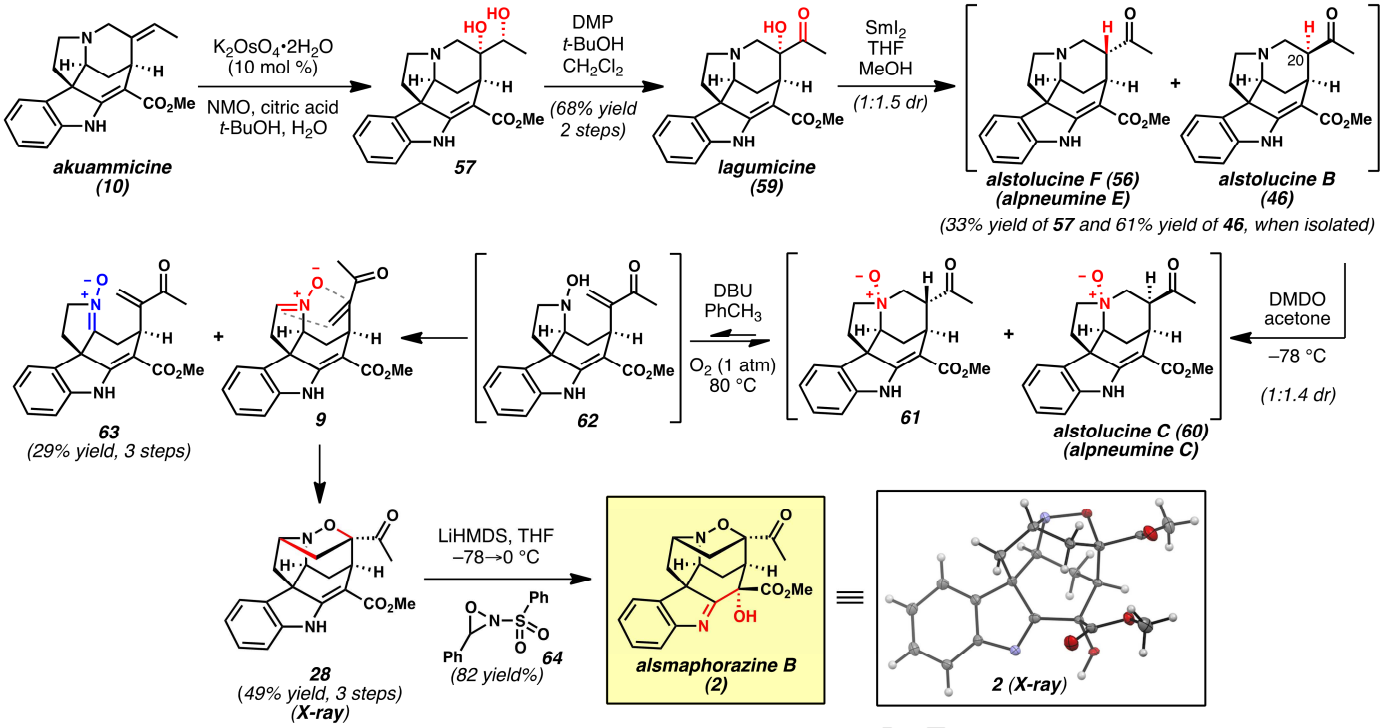

Scheme 15. Bioinspired Synthesis of *Alstonia* Alkaloids.

emulsions with particulate osmium. Oxidation of the secondary alcohol with Dess–Martin periodinane using *t*-BuOH as an accelerant[41] for this challenging substrate provided α-hydroxyketone lagumicine (**59**).[42] Other oxidants such as Jones, Swern, or Parikh–Doering oxidation were serviceable, but incomplete conversion and lower isolated yields were frequent problems. Subsequent deoxygenation of the α-hydroxyketone **59** with SmI_2[43] provided the elusive pentacyclic ketones[27,33b,d,44]: alstolucine B (**46**)[25,33i,j] and a racemic mixture **56** of alstolucine F[25,33i,j]/alpneumine E[26] in 1:1.5 dr. The diastereomeric ketones could be separated by flash column chromatography and individually characterized, but routinely we kept the mixture and proceeded because the C20-stereogenic center would be ablated at a later stage.

As a more direct alternative to the dihydroxylation/ketone oxidation sequence, we aimed to apply known Os[45]- and Ru[46]-catalyzed conditions for alkene ketohydroxylation for the direct conversion of akuammicine to lagumicine. Unfortunately, these conditions led to complex mixtures containing starting material, diols, ketoalcohols, or their corresponding *N*-oxides.

To return to our primary goal of preparing alsmaphorazine B, *N*-oxidation of the crude mixture of diastereomers by action of DMDO led to the corresponding *N*-oxides **61** and **60** (1:1.4 dr), of which alstolucine C[25]/alpneumine C[26] (**60**) are a pair of enantiomeric natural products. Again, while these compounds could be separated and characterized, the mixture was typically taken forward.

Our next goal was to effect an *N*-oxide fragmentation and cycloaddition cascade to afford the caged polycyclic framework of alsmaphorazine B (**2**). The planned fragmentation step found precedent in Ciganek's observation of $E1_{cb}$ elimination of an *N*-methyl *N*-oxide nipecotic ester derivative to a hydroxylamino enoate ester upon heating a under vacuum.[47] We reasoned that performing the elimination under air could lead to oxidation of the intermediate *N*-oxides for the second cycloaddition step. Treatment of the mixture of *N*-oxides **60** and **61** with DBU in toluene with mild heating in the presence of air as an oxidant provided some of the desired cycloadduct puzzlingly led also provided a mixture of deoxygenated ketones and the undesired nitrone isomer (Scheme 16). This net result potentially indicated a disproportionation of the *N*-oxide starting materials to a pair of reduced products and a pair of oxidized products, which was supported by TLC and NMR analysis during the reaction. Related redox processes have certainly been documented as undesired side reactions in Cope-type eliminations.[48] To circumvent this problem, we reasoned that a more strongly oxidizing atmosphere[49] would militate against the competing disproportionation process and drive the reaction toward oxidized nitrone products, one of which would afford the desired caged hexacyclic core. Conducting the reaction under a balloon of oxygen instead of air resulted in a cleaner product profile,

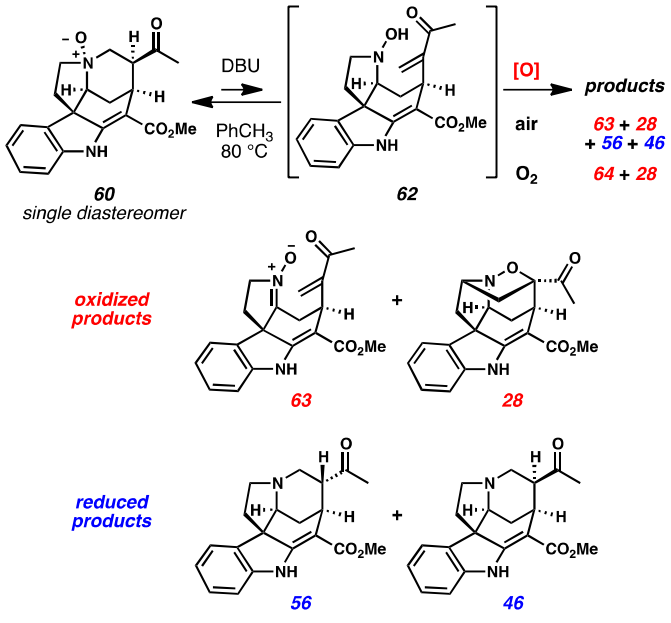

Scheme 16. Key Observations in Key 1,3-Dipolar Cycloaddition Step and Structural Elucidation.

wherein the major product **28** (49% yield over three steps) was likely formed via elimination to intermediate hydroxylamine (**62**), facile aerobic oxidation to nitrones (**63**) and (**9**), and a spontaneous 1,3-dipolar cycloaddition of the former. The cage-like architecture of cycloadduct **28**, which had proved particularly elusive to this point, was confirmed by X-ray crystallographic analysis of single crystals.

With only one oxidation separating our compound from the final target, we evaluated a number of oxidation conditions for the installation of the tertiary alcohol and indolenine moiety (Scheme 15).[50] An extensive survey of peroxide, peracid, and other oxidants led to complex mixtures of products, apparently triggered by oxidation of the electron-rich tertiary hydroxylamine. A second concern involved the potential sensitivity of the desired product **2** to further oxidation. With the clues from our unsuccessful initial experiments in hand, we recognized that deprotonation of the vinylogous carbamate would generate a much more electron-rich intermediate that should be subject to selective oxidation and also permit the use of milder, more chemoselective oxidants. Vinylogous carbamate lithiation with LiHMDS and oxidation with Davis oxaziridine (**64**) gratifyingly afforded (±)-alsmaphorazine B (**2**) in 82% yield. X-ray-quality crystals were obtained by vapor diffusion crystallization and provided conclusive confirmation of the alkaloid structure. The synthesis of this complex alkaloid was thus complete in over 10% overall yield from tryptamine.[51]

With our biogenetic hypothesis having yielded significant dividends in the reaction flask, we were able to take small detours to synthesize a number of related members of the family in one or two steps from the main route (Scheme 17). $NaBH_4$ reduction of alstolucine B (**46**) provided echitamidine (**64**),[27,33b,d,i,j,52] while the similar reduction of alstolucine F (**56**) in the presence of $CeCl_3 \cdot 7H_2O$ led to demethylalstogustine (**65**).[33b,d,i,j,34,53] Simple acylation of demethylalstogustine with ethyl chloroformate provided alstolucine A (**66**).[25,33i,j]

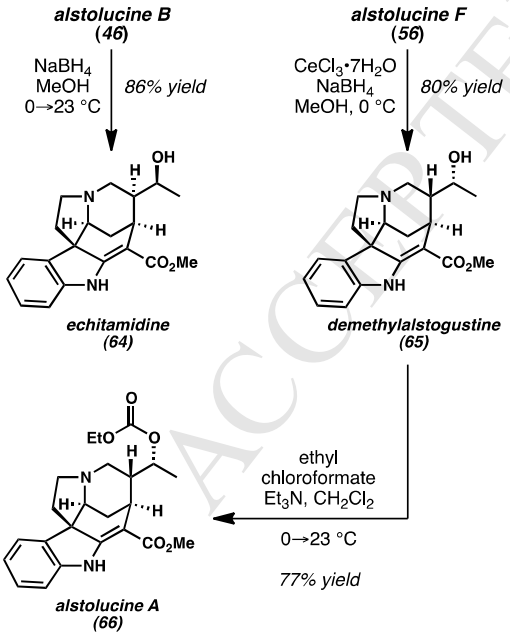

Scheme 17. Synthesis of Additional *Alstonia* Alkaloids.

While many of our initial strategies toward the alsmaphorazines proved discouraging, our patience was rewarded with a general synthetic route toward a broader natural product family from *Alstonia*, and permitted us to ascend the oxidation state ladder from akuammicine to alsmaphorazine B. Our synthetic work provides the basis for the synthesis of further oxidized members of the family such as alsmaphorazine A and oxidized analogues of the synthetic intermediates we have prepared along the way.

4. Conclusions

In summary, the success of our synthesis design for the alsmaphorazine alkaloids provides support for a possible biogenetic pathway from the common and less oxidized alkaloid akuammicine. Central to our strategy was the application of a formal [4+2] anionic bicyclization and a 1,3-dipolar cycloaddition, which together forged the hexacyclic skeleton. Key proposed oxidative manipulations and rearrangements proved more challenging than anticipated and we learned many important lessons about the innate reactivity of the highly functionalized, nitrogenous intermediates. Our determination was rewarded with a general approach that yielded akuammicine; akuammicine *N*-oxide; alstolucines A, B, C, and F; alpneumines C and E; lagumicine; echitamidine; demethylalstogustine; and alsmaphorazine B.

5. Experimental section

5.1. General Materials and Methods

All reactions were performed in oven-dried (140 °C) or flame-dried glassware under an atmosphere of dry argon unless otherwise noted. Reaction solvents including dichloromethane (CH_2Cl_2, Fisher, HPLC Grade), hexanes (Fisher, HPLC Grade), diethyl ether (Et_2O, Fisher, BHT stabilized, HPLC Grade), dimethylformamide (DMF, ACS Grade, Fisher), methanol (MeOH, low water, ACS Grade, Fisher), and tetrahydrofuran (THF, Fisher, HPLC Grade) were dried by percolation through a column packed with neutral alumina and a column packed with Q5 reactant, a supported copper catalyst for scavenging oxygen, under a positive pressure of argon.

Column chromatography was performed using EMD Millipore 60 Å (0.040–0.063 mm) mesh silica gel (SiO_2). Analytical thin-layer chromatography was performed on Merck silica gel 60 F_{254} TLC plates. Visualization was accomplished with UV (254 or 210 nm), and potassium permanganate ($KMnO_4$), *p*-anisaldehyde, ninhydrin, or 4-dinitrophenylhydrazine (DNPH) staining solutions.

^1H NMR and ^{13}C NMR spectra were recorded at 298 K on Bruker GN500 (500 MHz, ^1H; 125 MHz, ^{13}C), Bruker CRYO500 (500 MHz, ^1H; 125 MHz, ^{13}C), and Bruker AVANCE600 (600 MHz, ^1H) spectrometers. ^1H and ^{13}C spectra were referenced as follows for chloroform-*d* (7.26 ppm, ^1H; 77.00 ppm, ^{13}C) or methanol-d_4 (3.31 ppm, ^1H; 49.00, ppm ^{13}C). Chemical shifts are reported in ppm and multiplicities are indicated by: s (singlet), d (doublet), t (triplet), q (quartet), m (multiplet), and br s (broad singlet). Coupling constants, *J*, are reported in Hertz. Infrared (IR) spectra were recorded on a Perkin-Elmer spectrum RX1 FT-IR instrument or Varian 640-IR instrument on NaCl plates and peaks are reported in cm^{-1}. The raw fid files were processed into the included NMR spectra using MestReNova 10.0 (Mestrelab Research S.L.). Mass spectrometry data was obtained from the University of California, Irvine Mass Spectrometry Facility. High-resolution mass spectra (HRMS) were recorded on a Waters LCT Premier spectrometer using ESI-TOF (electrospray ionization-time of flight) and data are reported in the form of (*m/z*). Melting points (mp) were recorded on a Laboratory Devices Mel-Temp II melting point apparatus and are uncorrected.

Additional general information is available in the Supporting Information associated with this article.

5.2. Experimental Procedures and Characterization Data

Selected experimental procedures are shown below. A complete set of experimental procedures and characterization data for the new compounds described in this paper are available in the Supporting Information.

*5.2.1. N-Allyl Zincke Aldehyde **15a***

Freshly prepared *N*-allyl tryptamine (**16a**, 13.49 g, 67.38 mmol, 1.00 equiv), a brown-orange syrup, was added to a 500 mL round-bottom flask with magnetic stir bar and dissolved in CH_3CN (400 mL). The flask was cooled to 0 °C in an ice/water bath.

To a separate 250 mL flask with CH_3CN (200 mL) at 0 °C was added TFA (5.16 mL, 67.38 mmol, 1.00 equiv) dropwise by pipet. The flask was sealed with a rubber septum and the TFA solution was added to the reaction dropwise by positive pressure cannulation using a quadruple-layered Ar balloon over 30 min. The flask was sealed with a polypropylene cap and maintained at 0 °C.

Potassium salt **18**[8] (9.176 g, 67.38 mmol, 1.00 equiv) was added in one portion. The reaction became a heterogeneous sienna brown suspension. The solution phase became more red in color and less heterogeneous in consistency. After 2 h of stirring at 0 °C, the ice bath was removed and the reaction was allowed to slowly warm to ambient temperature.

After 6.5 h of stirring, the reaction was cooled to 0 °C and a solution of trifluoroacetic acid (516 μL, 6.78 mmol, 0.10 equiv) in CH_3CN (2 mL) was added dropwise, followed by potassium salt **18** (458 mg, 3.37 mmol, 0.05 equiv).

After an additional 3.5 h of stirring, the reaction was diluted with EtOAc (400 mL) and washed with brine (2 x 300 mL). The combined aqueous phases were extracted with EtOAc (2 x 200 mL). The combined organic phases were dried over Na_2SO_4, filtered, and concentrated under reduced pressure. The residue was purified by flash column chromatography (SiO_2, 12 x 12 cm, 20%→40%→50% acetone in hexane) to give Zincke aldehyde **15a**. The red-orange oil was sonicated in Et_2O until solids precipitated. The solids were filtered and washed with a small amount of cold Et_2O to give Zincke aldehyde **15a** (15.89 g, 56.50 mmol, 84% yield) as a pale brown solid. The filtrate was concentrated to give a red sap, which contained additional product with impurities.

The characterization data are identical to those previously reported by our group.[5b,d]

*5.2.2. N-Allyl Tetracyclic Enal **20a***

(Note: *Caution!* The reaction should be conducted behind a blast shield. The metallated indole is air-sensitive in solution and exclusion of air is essential to the success of the reaction. The enal product **20a** was stored under Ar in a –20 °C freezer as a precaution.)

To two oven-dried 350 mL sealable glass pressure vessels with magnetic stir bars were attached 24/40 septa. The flasks were further flame-dried under vacuum and cooled under double-layered Ar balloons. Zincke aldehyde **15a** (3.33 g, 11.88 mmol, 1.00 equiv), a yellow-orange powder was divided evenly between the two flasks (1.667 g each) and resealed with a rubber septum. The flasks were gently purged with Ar double-layered balloons through venting needles for 30 min.

Anhydrous THF (300 mL, degassed by sparging with Ar double-layered balloon in a sonicator for 1 h) was added to the pressure vessel containing Zincke aldehyde **15a** by positive pressure cannulation with a quadruple-layered Ar balloon.

KO*t*-Bu in THF (1.0 M, 7.49 mL, 7.49 mmol, 1.05 equiv) was added to each flask dropwise. The reactions became more turbid and darker orange. The 24/40 septa were quickly removed and replaced with Teflon screw caps with Teflon O-rings and Teflon tape-wrapped threads. The tightly-sealed flasks was immersed in preheated 80 °C oil baths. The reactions gradually developed a brown color over 20 min. The flasks were 25% immersed in the oil baths.

After 3 h 15 min of stirring, the flasks were cooled to ambient temperature. TLC analysis indicated consumption of starting material and appearance of product and *N*-allyl tryptamine **16a**. The brown turbid mixtures were quenched by cooling to 0 °C and poured into an ice-cold stirring mixture of sat. aq. $NaHCO_3$ (120 mL), EtOAc (250 mL), and H_2O (120 mL).

The phases were separated and the aqueous phases were extracted with EtOAc (3 x 100 mL). The combined organic phases were dried over Na_2SO_4, filtered, and concentrated under reduced pressure. The residue was purified by flash column chromatography (SiO_2, 7 x 20 cm, 10%→20%→30% acetone in hexanes) to give tetracyclic enal **20a** (4.47 g, 15.94 mmol, 67% yield) as a pale yellow-tan solid.

The characterization data are identical to those previously reported by our group.[5b,d]

*5.2.3. Akuammicine (**10**)*

To an oven and flame-dried 500 mL Schlenk flask with magnetic stir bar was added PPh_3 (746 mg, 2.842 mmol, 0.40 equiv) and vinyl iodide **30c** (3.20 g, 7.106 mmol, 1.00 equiv). The headspace was purged with a stream of Ar through a venting needle for 2 min. Et_3N (250 mL, sparged with Ar for > 1 h) was transferred into the flask by positive pressure cannulation, giving a yellow solution with insoluble white solids. The suspension was sonicated to break up the solids. The reaction was maintained under a double-layered Ar balloon.

$Pd(OAc)_2$ (320 mg, 1.421 mmol, 0.20 equiv) was quickly added in one portion with an Ar balloon counterflow. The Schlenk flask was sealed and immersed in a preheated 90 °C oil bath. The reaction clarified to a yellow solution and developed a darker orange color over time.

After 1 h of stirring, a suspension with a brown solution phase was observed with white solids deposited on the sides of the flask. After 2 h of stirring, the reaction was cooled to ambient temperature and carefully concentrated under reduced pressure. The residue was diluted with CH_2Cl_2 (100 mL) and washed with brine (200 mL). The aqueous phase was extracted with CH_2Cl_2 (3 x 100 mL) and the combined organic phases were dried over Na_2SO_4, filtered, and concentrated under reduced pressure.

The residue was purified by flash column chromatography (SiO_2, 98:1.9:0.2 → 96:3.6:0.4 → 94:5.4:0.6 → 92:7.2:0.8 → 90:9.0:1.0 CH_2Cl_2:MeOH:NH_4OH(*aq*)). The combined concentrated fractions containing akuammicine (**10**) were partitioned between CH_2Cl_2 (150 mL) and 1 M aq. NaOH (150 mL). The phases were separated and the aqueous phases were extracted with CH_2Cl_2 (3 x 50 mL). The combined organic phases were dried over Na_2SO_4, filtered, and concentrated under reduced pressure to provide akuammicine (**10**) (2.272 g, 7.048 mmol, 99% yield) as a pale orange solid.

^{1}H NMR (500 MHz, $CDCl_3$) δ 9.00 (br s, 1H), 7.22 (d, *J* = 7.4 Hz, 1H), 7.14 (dd, *J* = 7.7, 7.7 Hz, 1H), 6.89 (dd, *J* = 7.5, 7.5 Hz, 1H), 6.81 (d, *J* = 7.8 Hz, 1H), 5.34 (q, *J* = 7.1 Hz, 1H), 4.09–4.00 (m, 1H), 3.96–3.91 (m, 1H), 3.89 (d, *J* = 15.2 Hz, 1H), 3.80 (s, 3H), 3.27 (ddd, *J* = 12.6, 12.6, 5.6 Hz, 1H), 3.02 (dd, *J* = 12.4, 6.7 Hz, 1H), 2.95 (d, *J* = 15.1 Hz, 1H), 2.50 (ddd, *J* = 12.6, 12.6, 6.7 Hz, 1H), 2.41 (ddd, *J* = 13.5, 4.0, 2.2 Hz, 1H), 1.82 (dd, *J* = 12.4, 5.6 Hz, 1H), 1.60 (d, *J* = 6.9 Hz, 3H), 1.29 (d, *J* = 13.7, 3.0, 3.0 Hz, 1H); **^{13}C NMR** (125 MHz, $CDCl_3$) δ 168.1, 168.0, 143.5, 139.2, 137.0, 127.9, 121.0, 121.0, 120.9, 109.5, 101.4, 62.1, 57.7, 57.1, 56.4, 51.1, 46.4, 31.0, 29.9, 13.0; **IR** (Neat Film NaCl) 3363, 2946, 2863, 1669, 1602, 1477, 1464, 1435, 1383, 1311, 1274, 1237, 1203, 1160, 1133, 1100, 1073, 1056, 1018, 881, 855, 833, 802, 788, 746; **HRMS** (ES+) *m/z* calc'd for $C_{20}H_{24}N_2O_2$ $[M+H]^+$: 323.1760; found 323.1758; $\mathbf{R}_f$ = 0.41 (10% MeOH in CH_2Cl_2)

*5.2.4. Cycloadduct **28** and Nitrone **63***

(Note: During our early optimization of this reaction, we found that performing this reaction with a single diastereomer of *N*-oxide starting material (**60**) using a balloon of air instead of oxygen (with or without base) led to the formation of diastereomeric amino ketone natural products **46** and **56** along with cycloadduct **28**, nitrone **63**, and other minor products.)

To a 100 mL round-bottom flask with magnetic stir bar, alstolucine C / alpneumine C (**60**) (75.1 mg, 0.211 mmol, 1.00 equiv) was attached a 14/20 rubber septum. The flask was evacuated and backfilled with double-layered O_2 balloon (3 x). $PhCH_3$ (20 mL) was added by syringe. The mixture was sonicated to loosen the solids from the sides of the flask. DBU (95 μL, 0.636 mmol, 3.00 equiv) was added dropwise and the suspension clarified somewhat. Additional sonication was applied to help dissolve additional solids. The flask was immersed in a preheated 80 °C oil bath and stirred under a double-layered O_2 balloon. The solids gradually dissolved and the solution became more yellow in color.

After 18 h of stirring, the reaction was an orange solution with brown gummy residue visible on the flask walls. The reaction was cooled to ambient temperature and concentrated under reduced pressure. The brown residue was purified by flash column chromatography (SiO_2, 1%→2%→3%→4%→6% MeOH in CH_2Cl_2) to give cycloadduct **28** (30.4 mg, 0.0863 mmol, 41% yield) as a pale tan solid and nitrone **63** (8.7 mg, 0.0247 mmol, 28% yield) as a white solid.

Cycloadduct **28**: **^{1}H NMR** (500 MHz, $CDCl_3$) δ 9.04 (br s, 1H), 7.19 (d, *J* = 7.8 Hz, 1H), 7.16 (ddd, *J* = 7.7, 7.7, 1.1 Hz, 1H), 6.94 (ddd, *J* = 7.5, 7.5, 1.0 Hz, 1H), 6.83 (d, *J* = 7.8 Hz, 1H), 4.40–4.30 (m, 1H), 4.05 (ddd, *J* = 10.3, 6.2, 2.6 Hz, 1H), 3.77–3.33 (m, 1H), 3.76 (s, 3H), 2.52–2.43 (m, 2H), 2.44 (d, *J* = 14.0 Hz, 1H), 2.30 (s, 3H), 2.23 (dd, *J* = 13.8, 6.2 Hz, 1H), 2.16 (dd, *J* = 12.6, 10.3 Hz, 1H), 1.09 (br d, *J* = 12.7 Hz, 1H); **^{13}C NMR** (125 MHz, $CDCl_3$) δ 206.0, 167.3, 165.9, 144.3, 133.1, 128.6, 121.8, 121.7, 110.0, 100.2, 90.6, 66.3, 61.8, 56.0, 51.4, 43.7, 40.5, 34.4, 25.9, 25.7; **IR** (Neat Film NaCl) 3361, 3054, 2950, 2925, 2853, 2500, 1717, 1674, 1603, 1465, 1438, 1378, 1361, 1332, 1289, 1248, 1201, 1191, 1173, 1111, 1069, 1040, 969, 930, 897, 874, 824, 807, 787, 752, 737, 706; **HRMS** (ES+) *m/z* calc'd for $C_{20}H_{20}N_2O_4Na$ $[M+Na]^+$: 375.1321; found 375.1321; $\mathbf{R}_f$ = 0.35 (2:1 hexanes : acetone), 0.37 (5% MeOH in CH_2Cl_2); **mp** = 234–236 °C (acetone/pentane) (dec.)

Nitrone **63**: **^{1}H NMR** (500 MHz, $CDCl_3$) δ 9.03 (br s, 1H), 7.23 (dd, *J* = 7.7, 7.7 Hz, 1H), 7.20 (d, *J* = 7.7 Hz, 1H), 6.91 (dd, *J* = 7.7, 7.7 Hz, 1H), 6.90 (d, *J* = 7.7 Hz, 1H), 6.10–6.01 (m, 1H), 5.75–5.66 (m, 1H), 4.58–4.44 (m, 2H), 3.86 (dd, *J* = 13.3, 9.0 Hz, 1H), 3.71 (s, 3H), 3.38 (d, *J* = 13.6 Hz, 1H), 2.61 (ddd, *J* = 11.8, 11.8, 9.0 Hz, 1H), 2.43 (s, 3H), 2.20–2.06 (m, 2H); **^{13}C NMR** (125 MHz, $CDCl_3$) δ 199.7, 167.5, 166.4, 150.1, 144.9, 144.2, 131.5, 129.4, 125.3, 121.5, 121.5, 110.9, 100.3, 61.8, 57.8, 51.8, 39.9, 38.4, 28.2, 26.8; **IR** (Neat Film NaCl) 3214, 2922, 2852, 1740, 1731, 1679, 1592, 1555, 1464, 1437, 1360, 1331, 1314, 1280, 1264, 1236, 1205, 1184, 1168, 1084, 1054, 1032, 953, 800, 778, 752; **HRMS** (ES+) *m/z* calc'd for $C_{20}H_{20}N_2O_4Na$ $[M+ Na]^+$: 375.1321; found 375.1321; $\mathbf{R}_f$ = 0.33 (5% MeOH in CH_2Cl_2).

*5.2.5. Alsmaphorazine B (**2**)*

To a flame-dried 25 mL round-bottom flask charged with a magnetic stir bar and vinylogous carbamate **28** (10.0 mg, 0.028 mmol, 1.00 equiv) under an Ar balloon was added THF (4 mL). The solution was cooled to –78 °C in a CO_2(s)/acetone bath and stirred for 10 min.

A solution of LiHMDS (0.1 M in THF, 340 μL, 0.0340 mmol, 1.20 equiv) was added dropwise. The pale yellow-orange solution was stirred at –78 °C for 10 min. The cooling bath was removed and the reaction was allowed to warm to ambient temperature over 15 min and stirred for an additional 10 min.

The pale yellow solution cooled to –78 °C and stirred for 10 min. A solution of Davis oxaziridine **64** (14.8 mg, 0.0568 mmol, 2.00 equiv) in THF (0.5 mL) was added dropwise. The reaction was stirred at –78 °C and stirred for 10 min and the cooling bath was exchanged for an ice/water bath. The reaction became a turbid pale yellow solution within 2 min.

After 20 min of stirring at 0 °C, the reaction was quenched by the addition of sat. aq. $Na_2S_2O_3$ (2 mL) and brine (2 mL). The cooling bath was removed and the mixture was stirred for 5 min at ambient temperature. The mixture was extracted with CH_2Cl_2 (3 x 5 mL). The combined organic phases were dried over Na_2SO_4, filtered, and concentrated under reduced pressure. The residue was purified by flash column chromatography (SiO_2, 40%→60%→80%→100% EtOAc in hexanes) to give alsmaphorazine B (**2**) (8.6 mg, 0.023 mmol, 82% yield) as a white solid.

X-ray quality crystals of alsmaphorazine B (**2**) were grown by vapor diffusion crystallization (acetone/pentane) to give colorless translucent prisms.

^{1}H NMR (500 MHz, CD_3OD) δ 7.61 (d, *J* = 7.5 Hz, 1H), 7.42 (d, *J* = 14.3 Hz, 1H), 7.39 (dd, *J* = 7.5, 7.4 Hz, 1H), 7.35 (dd, *J* = 7.4, 7.2 Hz, 1H), 4.26–4.19 (m, 1H), 4.22–4.16 (m, 1H), 3.77 (s, 3H), 3.25–3.19 (m, 1H), 2.68 (dd, *J* = 14.4, 10.4 Hz, 1H), 2.54 (dd, *J* = 14.3, 6.6 Hz, 1H), 2.32 (s, 3H), 2.11 (d, *J* = 14.3 Hz, 1H), 2.05 (ddd, *J* = 14.1, 4.5, 4.5 Hz, 1H), 1.87 (dd, *J* = 14.5, 2.0 Hz, 1H), 1.21 (d, *J* = 14.1 Hz, 1H); **^{13}C NMR** (125 MHz, $CDCl_3$) δ 203.8, 186.2, 172.9, 153.6, 144.3, 129.7, 128.5, 123.2, 121.9, 90.2, 79.2, 68.2, 67.2, 64.1, 53.2, 45.4, 40.3, 39.4, 25.0, 19.0; **IR** (Neat Film NaCl) 3434, 3062, 2950, 1725, 1560, 1459, 1368, 1351, 1318, 1274, 1251, 1234, 1204, 1158, 1117, 1097, 1204, 1056, 1021, 900, 865, 826, 772, 735; **HRMS** (ES+) *m/z* calc'd for $C_{20}H_{20}N_2O_5Na$ $[M+Na]^+$: 391.1270; found 391.1270; $\mathbf{R}_f$ = 0.33 (2:1 hexanes : acetone); **mp** = 190–198 °C (acetone/pentane) (dec.) (the colorless crystals turn dark brown/black prior to melting, so chemical transformation may preclude state change).

Acknowledgments

Prof. David Martin and Lucas Nguyen are acknowledged for helpful insight and experimental advice. This work was generously supported by the NSF (CHE-1262040 and CHE-

1564340 to C.D.V) and an NIH NRSA Postdoctoral Fellowship (F32 GM103058 to A.Y.H.). We thank Profs. Larry Overman and Sergey Pronin for helpful discussions. Professor Toh-Seok Kam is acknowledged for providing copies of NMR spectra for alstolucine B, alstolucine C, and alstolucine F.

References and notes

1. Koyama, K.; Hirasawa, Y.; Nugroho, A. E.; Hosoya, T.; Hoe, T. C.; Chan, K.-L.; Morita, H. *Org. Lett.* **2010**, *12*, 4188−4191.
2. For computational studies of nitrone/alkene 1,3-dipolar cycloadditions in alkaloid biosynthesis, see: (a) Krenske, E. H.; Patel, A.; Houk, K. N. *J. Am. Chem. Soc.* **2013**, *135*, 17638−17642; (b) Painter, P. P.; Pemberton, R. P.; Wong, B. M.;Ho, K. C.; Tantillo, D. J. *J. Org. Chem.* **2014**, *79*, 432−435.
3. For recent total syntheses of alkaloids employing biomimetic nitrone-alkene 1,3-dipolar cycloadditions, see: (a) Miyatake-Ondozabal, H.; Bannwart, L. M.; Gademann, K. *Chem. Commun.* **2013**, *49*, 1921−1932; (b) Wei, H.; Qiao, C.; Liu, G.; Yang, Z.; Li, C.-c. *Angew. Chem., Int. Ed.* **2013**, *52*, 620−624; (c) Ma, N.; Yao, Y.; Zhao, B.-X.; Wang, Y.; Ye, W.-C.; Jiang, S. *Chem. Commun.* **2014**, *50*, 9284−9287.
4. (a) White, M. D.; Payne, K. A. P.; Fisher, K.; Marshall, S. A.; Parker, D.; Rattray, N. J; Trivedi, D. K.; Goodacre, R.; Rigby, S. E. J.; Scrutton, N. S.; Hay, S.; Leys, D. *Nature* **2015**, *522*, 502–506; (b) Payne, K. A. P.; White, M. D.; Fisher, K.; Khara, B.; Bailey, S. S.; Parker, D.; Rattray, N. J. W.; Trivedi, D. K.; Goodacre, R.; Beveridge, R.; Barran, P.; Rigby, S. E. J.; Scrutton, N. S.; Hay, S.; Leys, D. *Nature* **2015**, *522*, 497–501.
5. (a) Martin, D. B. C.; Vanderwal, C. D. *J. Am. Chem. Soc.* **2009**, *131*, 3472−3473; (b) Martin, D. B. C.; Vanderwal, C. D. *Chem. Sci.* **2011**, *2*, 649−651; (c) Vanderwal, C. D. *J. Org. Chem.* **2011**, *76*, 9555−9567; (d) Martin, D. B. C.; Nguyen, L. Q.; Vanderwal, C. D. *J. Org. Chem.* **2012**, *77*, 17−46.
6. (a) Zincke, T. *Justus Liebigs Ann. Chem.* **1903**, *330*, 361–374; (b) König, W. *J. Prakt. Chem.* **1904**, *69*, 105–137; (c) Zincke, T. *Justus Liebigs Ann. Chem.* **1904**, *333*, 296–345; (d) Zincke, T.; Würker, W. *Justus Liebigs Ann. Chem.* **1905**, *338*, 107–141.
7. Nolsøe, J. M. J.; Aursnes, M.; Tungen, J. E.; Hansen, T .V. *J. Org. Chem.* **2015**, *80*, 5377–5385.
8. (a) Nuhant, P.; Raikar, S. B.; Wypych, J.-C.; Delpech, B.; Marazano, C. *J. Org. Chem.* **2009**, *74*, 9413−9421; (b) Nguyen, T. M.; Peixoto, S.; Ouairy, C.; Nguyen, T. D.; Bénéchie, M.; Marazano, C.; Michel, P. *Synthesis* **2010**, 103−109.
9. Pham, H. V.; Martin, D. B. C.; Vanderwal, C. D.; Houk, K. N. *Chem. Sci.* **2012**, *3*, 1650–1655.
10. Corey, E. J.; Gilman, N. W.; Ganem, B. E. *J. Am. Chem. Soc.* **1968**, *90*, 5616–5617.
11. (a) Chan, A.; Scheidt, K. A. *Org. Lett.* **2005**, *7*, 905–908; (b) Sohn, S. S.; Bode, J. W. *Org. Lett.* **2005**, *7*, 3873–3876; (c) De Sarkar, S.; Grimme, S.; Studer, A. *J. Am. Chem. Soc.* **2010**, *132*, 1190–1191.
12. Gaspa, S.; Porcheddu, A.; De Luca, L. *Org. Lett.*, **2015**, *17*, 3666–3669.
13. Travis, B. R.; Sivakumar, M.; Olatunji Hollist, G.; Borhan, B. *Org. Lett.* **2003**, *5*, 1031–1034.
14. (a) Gopinath, R.; Patel, B. K. *Org. Lett.* **2000**, *2*, 577–579; (b) Talukdar, D.; Sharma, K.; Bharadwaj, S. K.; Thakur, A. J. *Synlett* **2013**, *24*, 963–966.
15. Zhang, Z.-W.; Yang, J. *Tetrahedron Lett.* **2014**, *55*, 761–763.
16. (a) Lindgren, B. O.; Nilsson, T. *Acta Chemica Scandinavica* **1973**, *27*, 888–890; (b) Kraus, G. A.; Taschner, M. J. *J. Org. Chem.* **1980**, *45*, 1175–1176; (c) Bal, B. S.; Childers, Jr., W. E.; Pinnick, H. W. *Tetrahedron* **1981**, *37*, 2091–2096.
17. Confalone, P. N.; Huie, E. M. *Org. React.* **1988**, *36*, 1−174.
18. (a) Shibasaki, M.; Boden, C. D. J.; Kojima, A. *Tetrahedron* **1997**, *53*, 7371–7395; (b) Beletskaya, I. P.; Cheprakov, A. V. *Chem. Rev.* **2000**, *100*, 3009–3066; (c) Dounay, A. B.; Overman, L. E. *Chem. Rev.* **2003**, *103*, 2945–2963; (d) Nicolaou, K. C.; Bulger, P. G.; Sarlah, D. *Angew. Chem. Int. Ed.* **2005**, *44*, 4442–4489.
19. Nilsson, P.; Larhed, M.; Hallberg, A. *J. Am. Chem. Soc.* **2003**, *125*, 3430–3431.
20. (a) McClure, K. F.; Danishefsky, S. J. *J. Am. Chem. Soc.* **1993**, *115*, 6094–6100; (b) Schkeryantz, J. M.; Danishefsky, S. J. *J. Am. Chem. Soc.* **1995**, *117*, 4722–4723; (c) Peng, J.; Lin, W.; Yuan, S.; Chen, Y. *J. Org. Chem.* **2007**, *72*, 3145–3148; (d) Hay. M. B. Wolfe, J. P. *Angew. Chem. Int. Ed.* **2007**, *46*, 6492–6494; (e) Lemen, G. S.; Giampietro, N. C.; Hay, M. B.; Wolfe, J. P. *J. Org. Chem.* **2009**, *74*, 2533–2540; (f) Al-Harassi, A.; Fischer, S.; Zimmer, R.; Reissig, H.-U. *Synthesis* **2010**, *2*, 304–314.
21. (a) Tufariello, J. J.; Mullen, G. B.; Tegeler, J. J.; Trybulski, E. J.; Wong, S. C.; Ali, Sk. A. *J. Am. Chem. Soc.* **1979**, *101*, 2435–2441; (b) Okue, M.; Kobayashi, H.; Shin-ya, K.; Furihata, K.; Hayakawa, Y.; Seto, H.; Watanabe, H.; Kitahara, T. *Tetrahedron Lett.* **2002**, *43*, 857–860; (c) Nagasawa, K.; Georgieva, A.; Koshino, H.; Nakata, T.; Kita, T.; Hashimoto, Y. *Org. Lett.* **2002**, *4*, 177–180; (d) Ishiwata, T.; Hino, T.; Koshino, H.; Hashimoto, Y.; Nakata, T.; Nagasawa, K. *Org. Lett.* **2002**, *4*, 2921–2924; (e) Nagasawa, K.; Ishiwata, T.; Hashimoto, Y.; Nakata, T. *Tetrahedron Lett.* **2002**, *43*, 6383–6385.
22. Berman, A. M.; Johnson, J. S. *J. Org. Chem.* **2006**, *71*, 219–224.
23. (a) Chakravarti, R. N.; Pausacker, K. H.; Robinson, R.; *J. Chem. Soc.* **1947**, 1554–1556; (b) Kuehne, M.; Xu, F. *J. Org. Chem.* **1993**, *58*, 7490–7497.
24. Buston, J. E. H.; Coldham, I.; Mulholland, K. R. *Tetrahedron: Asymmetry*. **1998**, *9*, 1995–2009.
25. Alstolucines isolation: Tan, S.-J.; Low, Y.-Y.; Choo, Y.-M.; Abdullah, Z.; Etoh, T.; Hayashi, M.; Komiyama, K.; Kam, T.-S. *J. Nat. Prod.* **2010**, *73*, 1891−1897.
26. Alpneumines isolation: Koyama, K.; Hirasawa, Y.; Hosoya, T.; Hoe, T. C.; Chan, K.-L.; Morita, H. *Bioorg. Med. Chem.* **2010**, *18*, 4415−4421.
27. Bonjoch, J.; Solé, D.; Bosch, J. *J. Am. Chem. Soc.* **1993**, *115*, 2064–2065.
28. During the course of our investigations, the Andrade group reported a similar strategy. See ref. 33j.
29. (a) Ge, H.; Niphakis, M. J.; Georg, G. I. *J. Am. Chem. Soc.* **2008**, *130*, 3708–3709; (b) Yu, Y.-Y.; Niphakis, M. J.; Georg, G. I. *Org. Lett.* **2011**, *13*, 5932–5935; (c) Gigant, N.; Gillaizeau, I. *Org. Lett.* **2012**, *14*, 3304–3307.
30. (a) Oppolzer, W.; DeVita, R. J. *J. Org. Chem.* **1991**, *56*, 6256–6257; (b) Oppolzer, W.; Bienayamé, H.; Genevois-Borella, A. *J. Am. Chem. Soc.* **1991**, *113*, 9660–9661; (c) Preindl, J.; Leitner, C.; Baldauf, S.; Mulzer, J. *Org. Lett.* **2014**, *16*, 4276−4279.
31. Rawal, V. H.; Michoud, C. *Tetrahedron Lett.* **1991**, *32*, 1695−1698.
32. Isolation and structure determination of akuammicine: (a) Millson, M. F.; Robinson, R.; Thomas, A. F. *Experientia* **1953**, *9*, 89−91; (b) Edwards, P. N.; Smith, G. F. *J. Chem. Soc.* **1961**, 152−156.
33. (a) Angle, S. R.; Fevig, J. M.; Knight, S. D.; Marquis, R. W., Jr.; Overman, L. E. *J. Am. Chem. Soc.* **1993**, *115*, 3966−3976; (b) Kuehne, M. E.; Xu, F.; Brook, C. S. *J. Org. Chem.* **1994**, *59*, 7803−7806; (c) Martin, S. F.; Clark, C. W.; Ito, M.; Mortimore, M. *J. Am. Chem. Soc.* **1996**, *118*, 9804−9805; (d) Bonjoch, J.; Solé, D.; García-Rubio, S.; Bosch, J. *J. Am. Chem. Soc.* **1997**, *119*, 7230−7240; (e) He, S. Ph.D. Dissertation (Rawal), University of Chicago, Chicago, IL, 2001; (f) Sirasani, G.; Paul, T.; Dougherty, W., Jr.; Kassel, S.; Andrade, R. B. *J. Org. Chem.* **2010**, *75*, 3529−3532; (g) Jones, S. B.; Simmons, B.; Mastracchio, A.; MacMillan, D. W. C. *Nature* **2011**, *475*, 183−188; (h) Munagala, S.; Sirasani, G.; Kokkonda, P.; Phadke, M.; Krynetskaia, N.; Lu, P.; Sharom, F. J.; Chaudhury, S.; Abdulhameed, M. D. M.; Tawa, G.; Wallqvist, A.; Martinez, R.; Childers, W.; Abou-Gharbia, M.; Krynetskiy, E.; Andrade, R. B. *Bioorg. Med. Chem.* **2014**, *22*, 1148−1155; (i) Teijaro, C. N.; Munagala, S.; Zhao, S.; Sirasani, G.; Kokkonda, P.; Malofeeva, E. K.; Hopper-Borge, E.; Andrade, R. B. *J. Med. Chem.* **2014**, *57*, 10383−10390; (j) Teijaro, C. N.; Zhao, S.; Kokkonda, P.; Andrade, R. B. *Synthesis* **2015**, *47*, 1547–1556.
34. Salim, A. A.; Garson, M. J.; Craik, D. J. *J. Nat. Prod.* **2004**, *67*, 1591–1594.
35. Castagnoli, Jr., N.; Cymerman Craig, J.; Melikian, A. P.; Roy, S. K. *Tetrahedron* **1970**, *26*, 4319–4327.
36. VanRheenen, V.; Kelly, R. C.; Cha, D. Y. *Tetrahedron Lett.* **1976**, *17*, 1973−1976.
37. Gilbert, B.; Duarte, A. P.; Nakagawa, Y.; Joule, J. A.; Flores, S. E.; Brissolese, J. A.; Campello, J.; Carrazzoni, E. P.; Owellen, R. J.; Blossey, E. C.; Brown, K. S., Jr.; Djerassi, C. *Tetrahedron* **1965**, *21*, 1141−1166.
38. Mirand, C.; Massiot, G.; Le Men-Olivier, L.; Lévy, J. *Tetrahedron Lett.* **1982**, *23*, 1257−1258.
39. (a) Applequist, D. E.; Gebauer, P. A.; Gwynn, D. E.; Hardy O'Connor, L. *J. Am. Chem. Soc.* **1972**, *94*, 4272–4278; (b) DeCamp, A. E.; Mills, S. G.; Kawaguchi, A. T.; Desmond, R.; Reamer, R. A.; DiMichele, L.; Volante, R. P. *J. Org. Chem.* **1991**, *56*, 3564–3571; (c) Defaut, B.; Parsons, D. B.; Spencer, N.; Male,

L.; Kariuki, B. M.; Grainger, R. S. *Org. Biomol. Chem.* **2012**, *10*, 4926–4932.
40. Dupau, P.; Epple, R.; Thomas, A. A.; Fokin, V. V.; Sharpless, K. B. *Adv. Synth. Catal.* **2002**, *344*, 421−433.
41. Dess, D. B.; Martin, J. C. *J. Org. Chem.* **1983**, *48*, 4155−4156.
42. Kam, T.-S.; Choo, Y.-M. *Phytochemistry* **2004**, *65*, 603–608.
43. (a) Molander, G. A.; Hahn, G. *J. Org. Chem.* **1986**, *51*, 1135−1138; (b) White, J. D.; Somers, T. C. *J. Am. Chem. Soc.* **1994**, *116*, 9912−9920; (c) Jiang, X.; Wang, C.; Hu, Y.; Hu, H.; Covey, D. F. *J. Org. Chem.* **2000**, *65*, 3555−3557.
44. Kuehne, M. E.; Brook, C. S.; Frasier, D. A.; Xu, F. *J. Org. Chem.* **1994**, *59*, 5977–5982.
45. (a) Murahashi, S.-I.; Naota, T.; Hanaoka, H. *Chem. Lett*. **1993**, 1767–1770; (b) Fleming, J. J.; McReynolds, M. D.; DuBois, J. *J. Am. Chem. Soc.* **2007**, *129*, 9964−9975; (c) Fleming, J. J.; McReynolds, M. D.; DuBois, J. *J. Am. Chem. Soc.* **2007**, *129*, 9964–9975.
46. (a) Plietker, B. *J. Org. Chem.* **2003**, *68*, 7123-7125; (b) Plietker, B.; Niggemann, M. *Org. Lett*. **2003**, *5*, 3353–3356. (c) Plietker, B. *J. Org. Chem.* **2003**, *68*, 7123-7125; (d) Plietker, B. *J. Org. Chem.* **2004**, *69*, 8287-8296; (e) Plietker, B.; Niggemann, M.; Pollrich, A. *Org. Biomol. Chem.* **2004**, *2*, 1116–1124; (f) Plietker, B. *Eur. J. Org. Chem.* **2005**, 1919–1929.
47. Ciganek, E.; Read, J. M., Jr.; Calabrese, J. C. *J. Org. Chem.* **1995**, *60*, 5795−5802.
48. Laughlin, R. G. *J. Am. Chem. Soc.* **1973**, *95*, 3295−3299.
49. Johnson, D. H.; Rogers, M. A. T.; Trappe, G. *J. Chem. Soc.* **1956**, 1093−1103.
50. (a) Hugel, G.; Massiot, G.; Lévy, J.; Le Men, J. *Tetrahedron* **1981**, *37*, 1369−1375; (b) Danieli, B.; Lesma, G.; Palmisano, G.; Riva, R. *J. Chem. Soc., Chem. Commun.* **1984**, 909−911; (c) Kuehne, M. E.; Podhorez, D. E.; Mulamba, T.; Bornmann, W. G. *J. Org. Chem.* **1987**, *52*, 347−353; (d) Kobayashi, S.; Ueda, T.; Fukuyama, T. *Synlett* **2000**, 883−886; (e) Nemes, A.; Szántay, C., Jr.; Czibula, L.; Greiner, I. *Heterocycles* **2007**, *71*, 2347−2362.
51. For the initial report of the alsmaphorazine B synthesis, see: Hong, A. Y.; Vanderwal, C. D. *J. Am. Chem. Soc.* **2015**, *137*, 7306−7309.
52. Zeches, M.; Ravao, T.; Richard, B.; Massiot, G.; Le Men-Olivier, L. *Tetrahedron Lett.* **1984**, *25*, 659–662.
53. Tan, S.-J.; Low, Y.-Y.; Choo, Y.-M.; Abdullah, Z.; Etoh, T.; Hayashi, M.; Komiyama, K.; Kam, T.-S. *J. Nat. Prod.* **2010**, *73*, 1891–1897.

Supplementary Material

Supplementary data (experimental protocols and characterization data for key compounds) associated with this article can be found, in the online version, at http://dx.doi.org/10.1016/j.tetlet.XXXX.